Cell Biochem Biophys (2016) 74:157–173
DOI 10.1007/s12013-016-0731-z

ORIGINAL PAPER

Comparative Structural Dynamics of tRNA^{Phe} with Respect to Hinge Region Methylated Guanosine: A Computational Approach

Kailas D. Sonawane[1,2] · Rohit S. Bavi[1,3] · Susmit B. Sambhare[1] · Prayagraj M. Fandilolu[1]

Received: 13 December 2014 / Accepted: 1 May 2016 / Published online: 23 May 2016

Abstract Transfer RNAs (tRNAs) contain various uniquely modified nucleosides thought to be useful for maintaining the structural stability of tRNAs. However, their significance for upholding the tRNA structure has not been investigated in detail at the atomic level. In this study, molecular dynamic simulations have been performed to assess the effects of methylated nucleic acid bases, N^2-methylguanosine (m^2G) and N^2-N^2-dimethylguanosine (m^2_2G) at position 26, i.e., the hinge region of *E. coli* tRNA^{Phe} on its structure and dynamics. The results revealed that tRNA^{Phe} having unmodified guanosine in the hinge region (G26) shows structural rearrangement in the core of the molecule, resulting in lack of base stacking interactions, U-turn feature of the anticodon loop, and TΨC loop. We show that in the presence of the unmodified guanosine, the overall fold of tRNA^{Phe} is essentially not the same as that of m^2G26 and m^2_2G26 containing tRNA^{Phe}. This structural rearrangement arises due to intrinsic factors associated with the weak hydrogen-bonding patterns observed in the base triples of the tRNA^{Phe} molecule. The m^2G26 and m^2_2G26 containing tRNA^{Phe} retain proper three-dimensional fold through tertiary interactions. Single-point energy and molecular electrostatics potential calculation studies confirmed the structural significance of tRNAs containing m^2G26 and m^2_2G26 compared to tRNA with normal G26, showing that the mono-methylated (m^2G26) and dimethylated (m^2_2G26) modifications are required to provide structural stability not only in the hinge region but also in the other parts of tRNA^{Phe}. Thus, the present study allows us to better understand the effects of modified nucleosides and ionic environment on tRNA folding.

Keywords tRNA · Modified nucleosides · N^2-methylguanosine (m^2G) · N^2,N^2-dimethylguanosine (m^2_2G) · Molecular dynamic simulations

✉ Kailas D. Sonawane
kds_biochem@unishivaji.ac.in

[1] Structural Bioinformatics Unit, Department of Biochemistry, Shivaji University, Kolhapur, Maharashtra (M.S.) 416 004, India

[2] Department of Microbiology, Shivaji University, Kolhapur, Maharashtra (M.S.) 416 004, India

[3] Present Address: Computational Biology and Bioinformatics Lab (CBBL), Department of Biochemistry, Gyeongsang National University, jinju, South Korea

Introduction

Post-transcriptional modifications of RNA nucleotides occur in all cells [1]. Such modifications are known to provide structural stability across the wide range of temperature in archaea as well as bacteria [2]. The nature of nucleoside modification in tRNA is considerably varied from, simple base or ribose methylation, base isomerization, base reduction, base thiolation, and more complex hypermodifications [3, 4]. An important characteristic of tRNA is the presence of high content of modified nucleosides of which methylation represents the principal post-transcriptional modification during its maturation. The modified nucleosides N^2-methylguanosine (m^2G) and N^2-N^2 dimethylguanosine (m^2_2G) are conserved at only two locations: at position 10 proximal dihydrouridine stem and at position 26 in the bend between the dihydrouridine (D) stem and anticodon stem (Fig. 1), where they play a vital role in the control and stabilization of the tertiary L-fold structure of the tRNA [5, 6]. The N^2-methylguanosine and N^2-N^2 dimethylguanosine modifications in

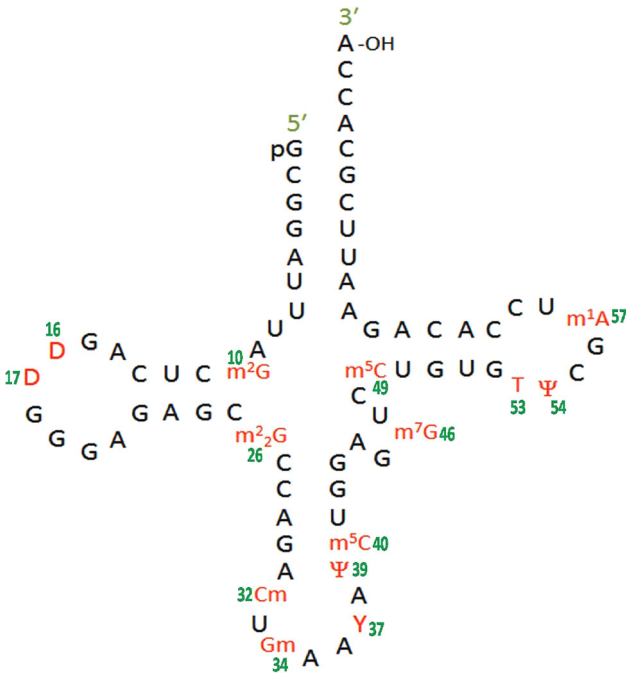

Fig. 1 Cloverleaf representation of yeast $tRNA^{Phe}$ secondary structure. *Red color* indicates modified nucleotides, and they are abbreviated as m^2G, N^2-methylguanosine; D, dihydrouridine; m^2_2G, N^2,N^2-dimethylguanosine; Cm, 2′-*O*-methylcytidine; Gm, 2′-*O*-methylguanosine; Y, wybutosine; ψ, pseudouridine; m^5C, 5-methylcytidine; m^7G, 7-methylguanosine; m^1A, 1-methyladenosine. Some of the residue numbers shown in *green color* (Color figure online)

tRNA are found not only at position 26 but also at positions 6, 7, 9, 10, 18, and 27 in several organisms [7]. X-ray crystallographic data of yeast $tRNA^{Phe}$ show that N^2,N^2-dimethylguanosine functions as a molecular hinge, adjusting the angular disposition of two stems within the tRNA architecture [8–10]. The main function of N^2,N^2-dimethylguanosine at position 26 is to maintain a certain amount of rigidity/flexibility in this part of the tRNA [9]. The NMR study describes the Watson–Crick base pairing between m^2_2G26:A44 and its role in tRNA folding [11]. Incorporation of m^2G was found to be iso-energetic with G in the duplex context as well as in GNRA (N = any nucleotide and R = purines) tetra loops [12]. The two rotamers of m^2G, *s-cis*, and *s-trans* have been found to be equally stable in RNA duplex [12] and in tRNA [13, 14]. It has been reported that the methylated guanosine present at the 26th position of tRNA regulates the stacking interactions and conformational dynamics [15].

It has also been proven that individual modifications allow tRNA to perform its biological activities in proper manner [16]. Nonetheless, it is usually thought that modifications found outside the anticodon loop help maintain the structural integrity of tRNA, while modifications within and around the anticodon are suggested to play a direct role in increasing translational efficiency and/or fidelity [17, 18]. Modified bases increase stability of tRNA structure by providing extra hydrogen bonding, enhance base stacking, and metal ion-binding interactions [19–26]. Previous studies on unmodified yeast $tRNA^{Phe}$ showed that Mg^{2+} was crucial in formation of tertiary structure, but removal of posttranscriptional modified nucleotide significantly altered the intrinsic stability of tertiary structure [27]. However, the mode in which posttranscriptional modifications exert their stabilizing effects on both secondary and tertiary structure is not completely understood. The effect of nonstandard bases on both structure and function can be verified after comparing the properties of "unmodified" tRNAs with the corresponding native tRNAs [27]. The influence of hydration effect on the dynamics of tRNA and lysozyme has been studied previously [28]. This study demonstrates that biomolecules with different chemical structures exhibit significant different dynamic responses to the water hydration [28]. Similarly, results of nucleic acids obtained using explicit solvent molecular dynamic (MD) simulations has been discussed thoroughly in a review published recently [29]. Conformational motion during spontaneous translocation has also been investigated using molecular dynamic (MD) simulation technique [30].

Hence, in the present study, multiple molecular dynamic simulations have been carried out in order to get structural and dynamic information of three fully solvated tRNAs. First, the level of convergence achieved by these trajectories is estimated by analysis of time-dependent root-mean-square deviations (RMSD) from the starting structure. Then, a detailed evaluation of the stability of the tertiary interactions, including base triples, tertiary base pairs, U-turn motifs of the anticodon loop and TΨC loop, including analysis of RMSF is presented.

Materials and Methods

Computational Procedures

The starting coordinates were extracted from the $tRNA^{Phe}$ A-form crystal structure [8] having 2.7 Å resolution (NDB code tRNA04; PDB code 6TNA). Transfer RNA molecule containing a total of 76 nucleotide bases has been surrounded by 75 Na^+ counter ions and 24599 SPC/E water molecules filling a 98.436 × 77.891 × 119.727 Å rectilinear box [31] with water density 1.0. Mg^{2+} ions were placed as observed in crystallographic symmetry [8]. Parameter files for Mg^{2+} ions were obtained from AMBER parameter database [32]. The MD simulations were performed by means of Amber ff99bsc0 force field [33] as implemented in AMBER 10 package, under periodic boundary conditions by employing Particle Mesh Ewald (PME) method [34] for the calculation of long-range

electrostatic interactions. MD trajectories were propagated at 2.0-fs time step applying the shake algorithm [35] to all hydrogen atoms with nonbonded cutoff of 9 Å. The nonbonded pair list was updated every 10 steps. The trajectories were calculated by maintaining constant temperature of 300 K and pressure (1 atm) at 2-fs time step, according to Berendsen coupling algorithm [36]. Equilibration protocol was kept similar to earlier MD simulation studies of nucleic acids [37, 38]. The equilibration protocol consisted of 5000 steps of steepest descent minimization followed by 20 ps of MD at 300 K applied for the relaxation of the initial strain present between water molecules and tRNA with m_2^2G at the 26th position. In the next step, tRNA was fixed, while water molecules and Na^+ counter ions were allowed to relax at 100 K (10 ps), 200 K (10 ps), and finally at 300 K for 960 ps, and thus equilibration protocol was completed at 1 ns. Equilibrated system was further subjected to 5000 steps of energy minimization using the steepest descent method in order to remove bad contacts between water molecules and tRNA. In further steps of MD simulation, no positional constraints were applied to the system, and the temperature was progressively increased to 300 K in steps of 50 K with 1 ps at every time step. Finally, system was subjected to production run of 10 ns at 300 K temperature and 1 atm constant pressure using fully solvated and neutralized system. Similar protocol has been applied for tRNA with N^2-N^2 dimethylguanosine (m_2^2G), N^2-methylguanosine (m^2G) base modifications, and unmodified guanosine at the 26th position, respectively.

The amber force field parameters for the naturally occurring modified nucleosides of tRNA were obtained from SantaLucia laboratory [39]. Visualization and the analyses of root-mean-square deviation (RMSD), root-mean-square fluctuation (RMSF), and the percentage of hydrogen bonding in tRNA were carried out using the VMD and PTRAJ module of Amber Tool 10, respectively [40]. Previously, various computational techniques have been used to understand the conformational behavior and dynamics of many complex, modified nucleosides [41–49]. Single-point energy calculations and molecular electrostatics potential (MEPs) calculations were performed using HF-SCF (6-31G** basis set) method as per previous study [43].

The dynamic stability of the unmodified and modified nucleic acid base pairs is important to retain the tertiary structure of a macromolecule (Fig. 2) and is indeed one of the best available criteria for valuing the quality of MD trajectory. This stability has been estimated by calculating hydrogen-bonding percentages (HB %) similarly as explained by Auffinger and coworkers in 1999 [50].

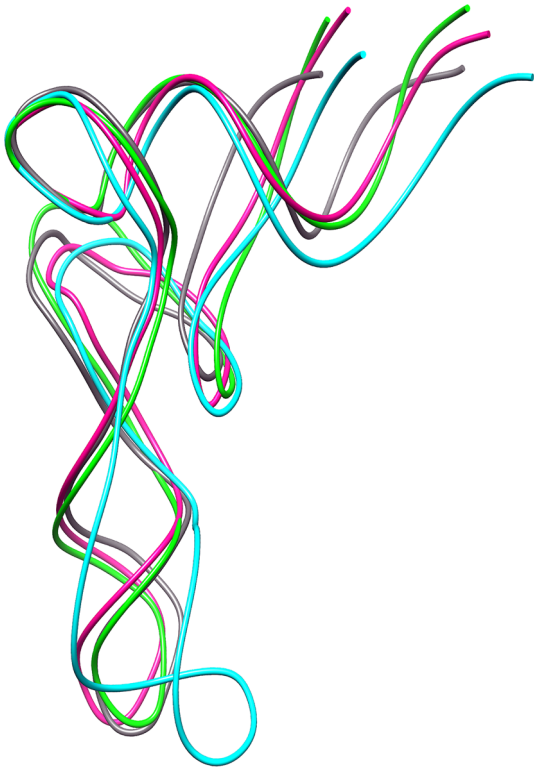

Fig. 2 Difference in conformation between unmodified guanosine (G26) and modified guanosine (m^2G26/m_2^2G26) in tRNAs. Superposition of average structures obtained after MD simulations; unmodified tRNA (unmodified guanosine; *cyan*), modified tRNA having m^2G (*magenta*), m_2^2G (*green*) at the 26th position, and $tRNA^{Phe}$ crystal structure with Mg^{2+} (*gray*, PDB ID 6TNA) (Color figure online)

Results

Stability of Intramolecular Hydrogen Bonds

The HB % are defined as the time over which a hydrogen bond fulfills the two d(H….O) < 2.5 Å and θ (X–H….O) > 135° standard criteria divided by the total simulation time (10 ns) as per earlier study [50]. The HB % results are described in Figs. 3, 4, 5, and 6.

Base Triples

Four base triples are found in the core of the tRNA, i.e., G45….[m^2G10-C25], m^7G46….[C13-G22], A9….[U12-A23], and A21….[U8-A14A]. The G45…. m^2G10-C25] base triple (Fig. 3) is involved in the interaction of the variable loop with the D stem, remains planar during the molecular dynamic simulation of crystal structure and also in the presence of guanosine (G), N^2-methylguanosine (m^2G), and N^2-N^2 dimethylguanosine (m_2^2G) at the 26th position of tRNA, respectively. The interaction involving the third base of the base triples is considered to be less

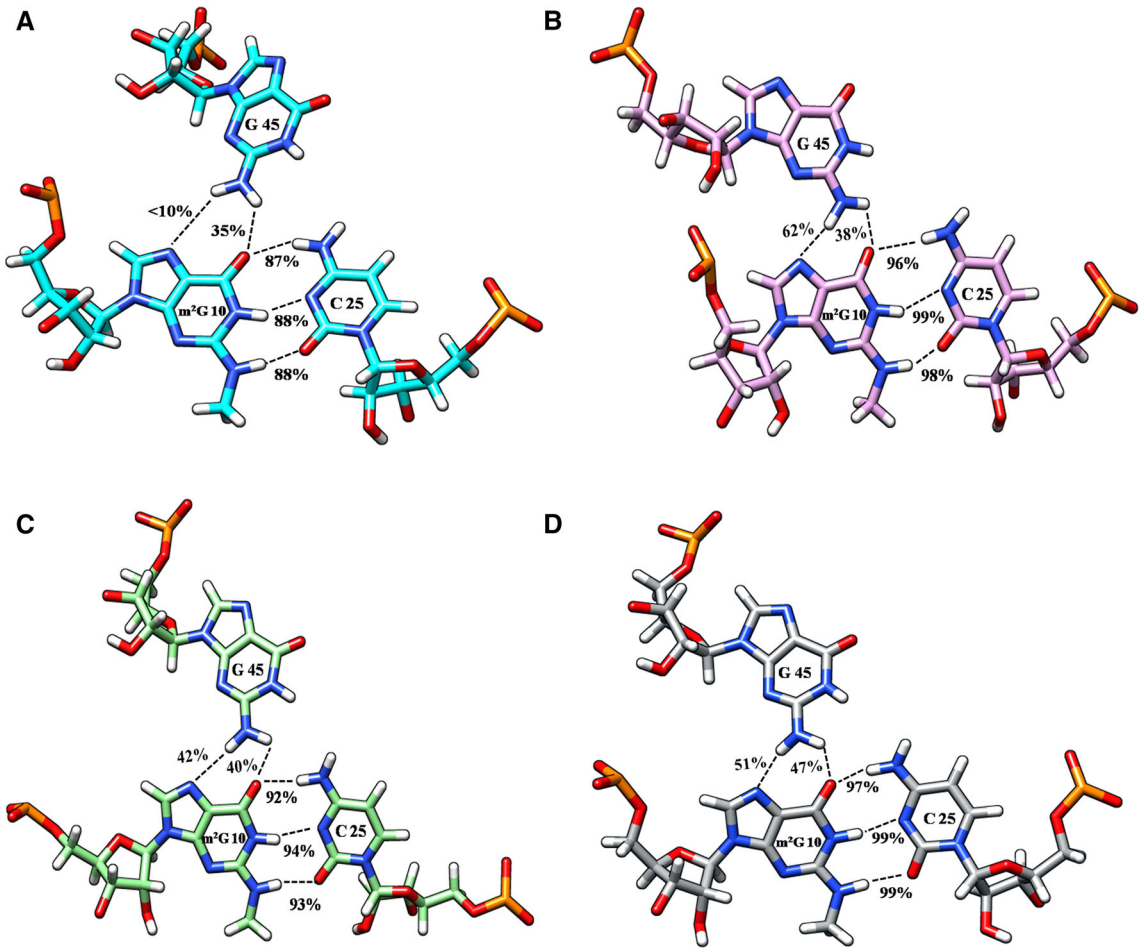

Fig. 3 The rearrangement of base triples G45….[m^2G10-C25]. **a** The base triples in the unmodified tRNA compared with **b** the base triples in m^2G containing tRNA, **c** the base triples in m_2^2G containing tRNA, and **d** the base triples in crystal structure with Mg^{2+} ions. HB % calculated from the 10-ns MD simulation for the base triples

stable for G compared with m^2G, m_2^2G, and crystal structure (Fig. 3a). It is worth noting that the base pairs forming hydrogen bonds display different levels of stability. In the core of tRNA, the A9….[U12-A23] (Fig. 4), A21….[U8-A14] (Fig. 5) and m^7G46….[C13-G22] (Fig. 6) base triple lose their planarity (Figs. 4a, 5a, 6a) during MD simulation in the presence of guanosine at the 26 position, while in the presence of N^2-methylguanosine (m^2G) (Figs. 4b, 5b, 6b) and N^2-N^2 dimethylguanosine (m_2^2G) (Figs. 4c, 5c, 6c), it prevents the loss of planarity. The presence of unmodified guanosine at the 26th position could be responsible for the loss of interaction between third base [A9] and base pair [U12-A23] forming the base triple; instead, A9 establishes a triple interaction with [C11-G24] base pair as observed in Fig. 7. The newly formed base triple is characterized by the hydrogen bond between (A9) N(6)H…O (6)(G24) and (A9) N(7)…HN(4) (C11) (Fig. 7a). Such displacement shifts m^7G46 toward U12–A23 base pair and forms hydrogen bond between (m^7G46) O6…HN6 (A23). Ultimately, the A21….[U8-A14] base triple involved in the trans Hoogsteen base pair between U8-A14 resulted in weak hydrogen bond with third base A21 as shown in Fig. 5. Besides base–base interactions, two base-sugar hydrogen bonds, i.e., (U8) O2′-H…N1 (A21) and (U8) O2′…H-N6 (A21), have been found during MD simulations. Such base-sugar hydrogen bond ((U8) O2′-H…N1 (A21)) was also observed in $tRNA^{Asp}$ [50] and $tRNA^{Phe}$ [51, 52] structures. This displacement of base triples in the tRNA core is the important structural event observed during molecular dynamic simulation in the presence of guanosine at the 26th position, while in the presence of N^2-methylguanosine (m^2G), N^2-N^2 dimethylguanosine (m_2^2G) and in crystal structure, no such displacement were observed. Thus, tertiary interaction may be related to the ionic environment of the tRNA and the presence of Mg^{2+} ions.

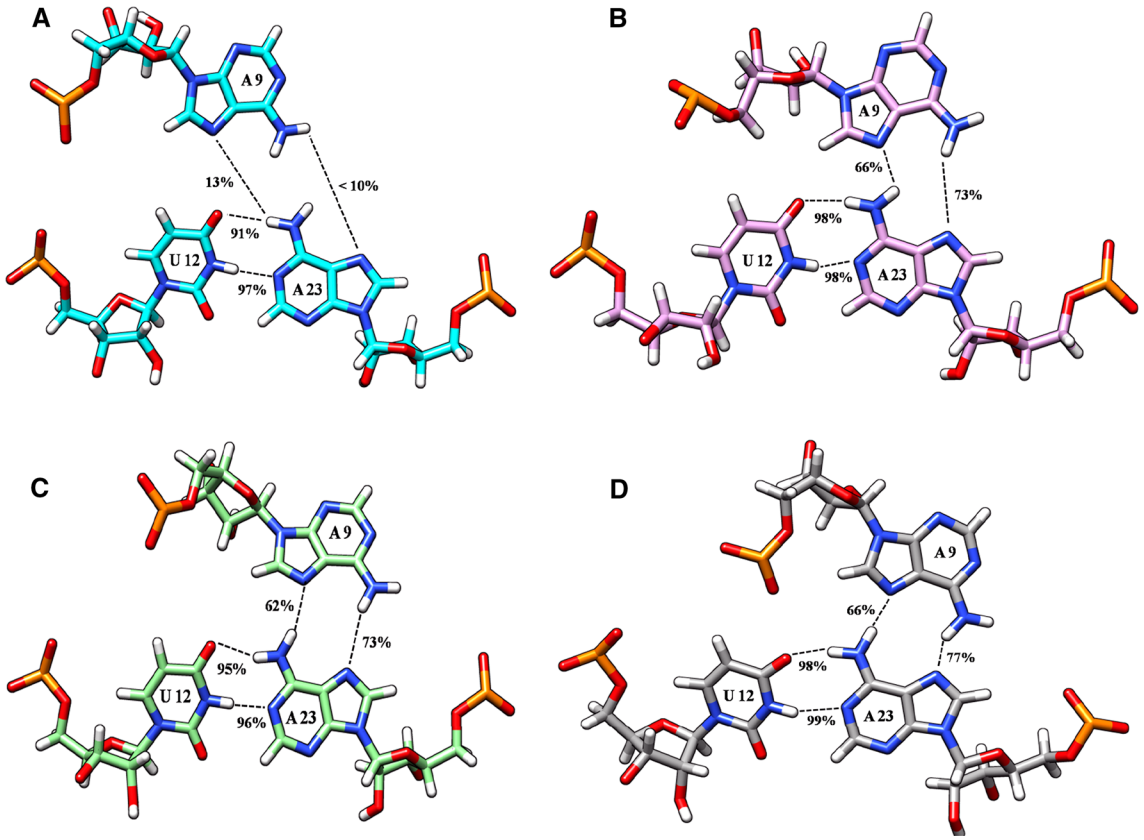

Fig. 4 The rearrangement of base triples A9….[U12-A23]. **a** The base triples in the unmodified tRNA compared with **b** the base triples in m^2G containing tRNA, **c** the base triples in m_2^2G containing tRNA, and **d** the base triples in crystal structure with Mg^{2+} ions. HB % calculated from the 10-ns MD simulation for the base triples

Tertiary Base Pairs

Besides the stem base pairs and base triples, extensive set of tertiary interactions are present in phylogenetically conserved bases of tRNAs, which are required to retain their complex three-dimensional structure [6, 52]. One of the important tertiary base pair present in tRNA is G26-A44 interaction. The derivatives of Guanosine nucleosides N^2-methylguanosine (m^2G) and N^2-N^2 dimethylguanosine (m_2^2G) have also been found at position 26, the junction between the D-stem and the anticodon stem, where they play a crucial role in stabilizing the continuity of interactions from the D stem to the anticodon stem. Hence, the basic idea lies in monitoring the effect of base pairing (G26/m^2G26/m_2^2G26:A44) on structural stability of tRNA during molecular dynamic simulation. The tertiary base pairs are properly maintained during 10-ns MD simulation trajectory of $tRNA^{Phe}$ crystal structure (Fig. 8d), as well as tRNAs containing m^2G (Fig. 8b) and m_2^2G (Fig. 8c). The O6….H-N6 hydrogen bond across the hinge region is especially well preserved in crystal structure, m^2G and with some variations for m_2^2G containing tRNA with HB % of 98, 98, and 87, respectively. The percentage of hydrogen bond between N1-H….N1 is 97 for crystal structure, 97 for m^2G, and 89 for m_2^2G. The difference in HB % of m_2^2G26:A44 may be due to the hydrophobic effect induced by $–CH_3$ group and also the orientation of methyl group, which changes from planar to propeller type conformation. The base pair between m_2^2G26:A44 do not just prevent the base pairing of G26 with C44 in the hinge region of tRNA, but also controls the pairing mode with A44. Thus, N^2,N^2-dimethylguanosine rules out the common sheared orientation between guanosine and adenosine. This has helped to bind this pairing mode to the more stable imino-hydrogen bonded form. There is a destabilization of loop due to loss of hydrogen bonding between G26-A44. The percentage of hydrogen bond, calculated between (G26) N1-H….N3 (A44) and (G26) O6….H-N6 (A44) is less than 10 % (Fig. 8a) resulting in loss of base stacking and destabilization of loop. It is worth noting that the percentage of hydrogen bonds forming these tertiary base pairs displays different levels of stability.

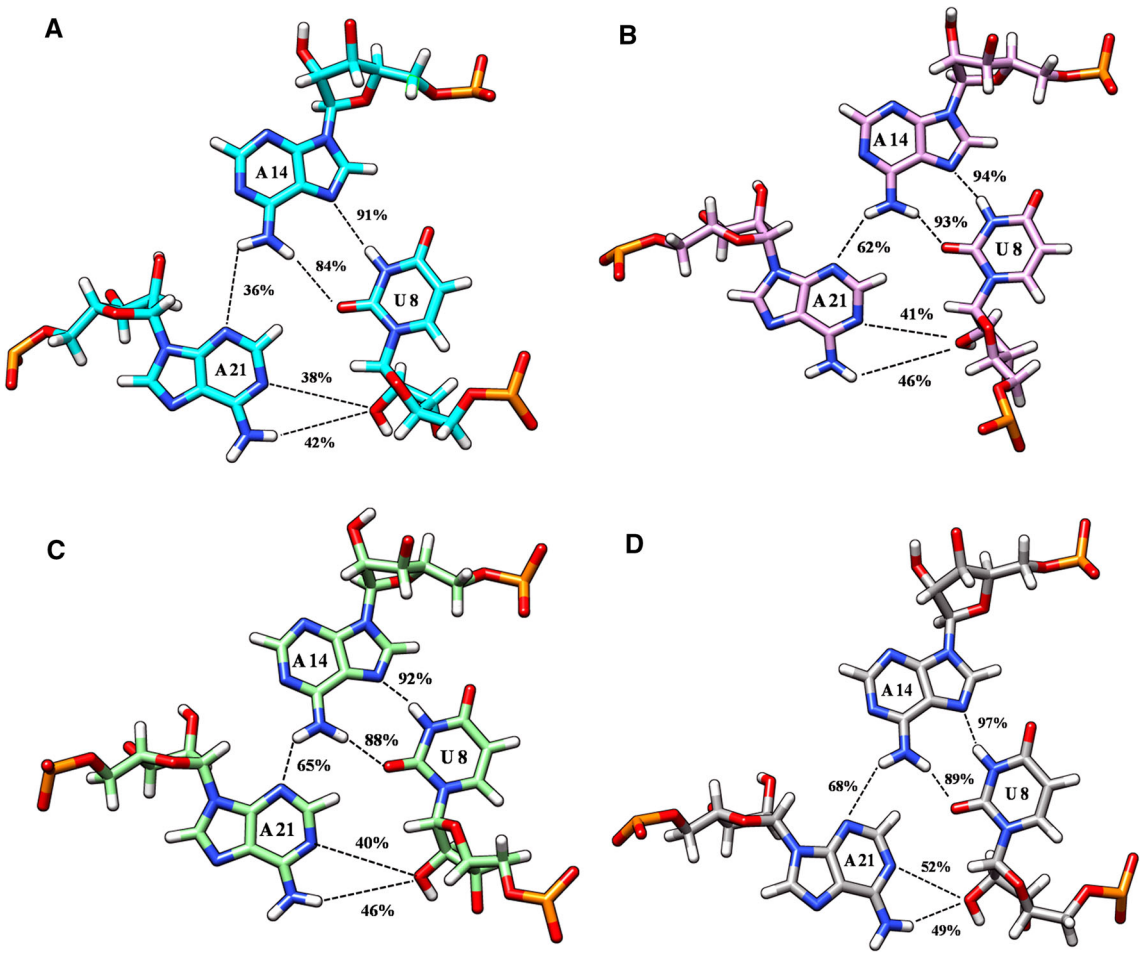

Fig. 5 The rearrangement of base triples A21….[U8-A14]. **a** The base triples in the unmodified tRNA compared with **b** the base triples in m^2G containing tRNA, **c** the base triples in m_2^2G containing tRNA, and **d** the base triples in crystal structure with Mg^{2+} ions. HB % calculated from the 10-ns MD simulation for the base triples

Effect of Hinge Region Modification on the Anticodon Loop and TΨC Loop

In tRNA structure, two base backbone interactions comprising the invariant U33 and Ψ55 residues maintain the U-turn of anticodon loop and thymine loop, respectively. Proper conformation of U33 nucleoside is crucial not only for a functional anticodon U-turn, but also for U-turn motifs in RNA structures in general. The (U33) N3-H…O2P (A36) hydrogen bond across the anticodon loop is particularly well conserved in crystal structure and m^2G containing tRNA (Fig. 9). However, tRNA having m_2^2G at the 26th position does not maintain the U-turn motif for initial 800 ps, which later gets stabilized as can be seen in Fig. 9. Destabilization of the U-turn motif has been observed in the anticodon loop of tRNA containing unmodified guanosine at the 26th position during molecular dynamic simulation (Fig. 9). However, the similar (Ψ55) N3-H…O2P(A58) interaction across the thymine loop breaks after 1400 ps due to dynamic rearrangements observed in tRNA having guanosine (G) at position 26 as compared to m^2G and m_2^2G containing tRNAs (Fig. 10). This kind of stable hydrogen-bonding interaction is also observed in crystal structure.

As per crystal structure analysis of yeast $tRNA^{Phe}$, G18 and G19 of D stem are involved in the formation of tertiary interactions with the bases Ψ55 and C56 of the TΨC domain, respectively [53]. The Base pair G18-Ψ55 stabilizes the interaction between D loop and TΨC loop which could have a possible role in interloop opening mechanism during protein synthesis process as discussed in previous study [54]. The O4 of Ψ55 forms bifurcated hydrogen-bonding interactions with N2 and N1 of G18 in $tRNA^{Phe}$ crystal structure [53] containing m^2G and m_2^2G as shown in Fig. 11. The tRNA with unmodified guanosine (G) does not hold such bifurcated hydrogen-bonding interactions resulted in destabilization of the bond that holds the D domain with TΨC domain (Fig. 11). The $tRNA^{Asp}$ has an

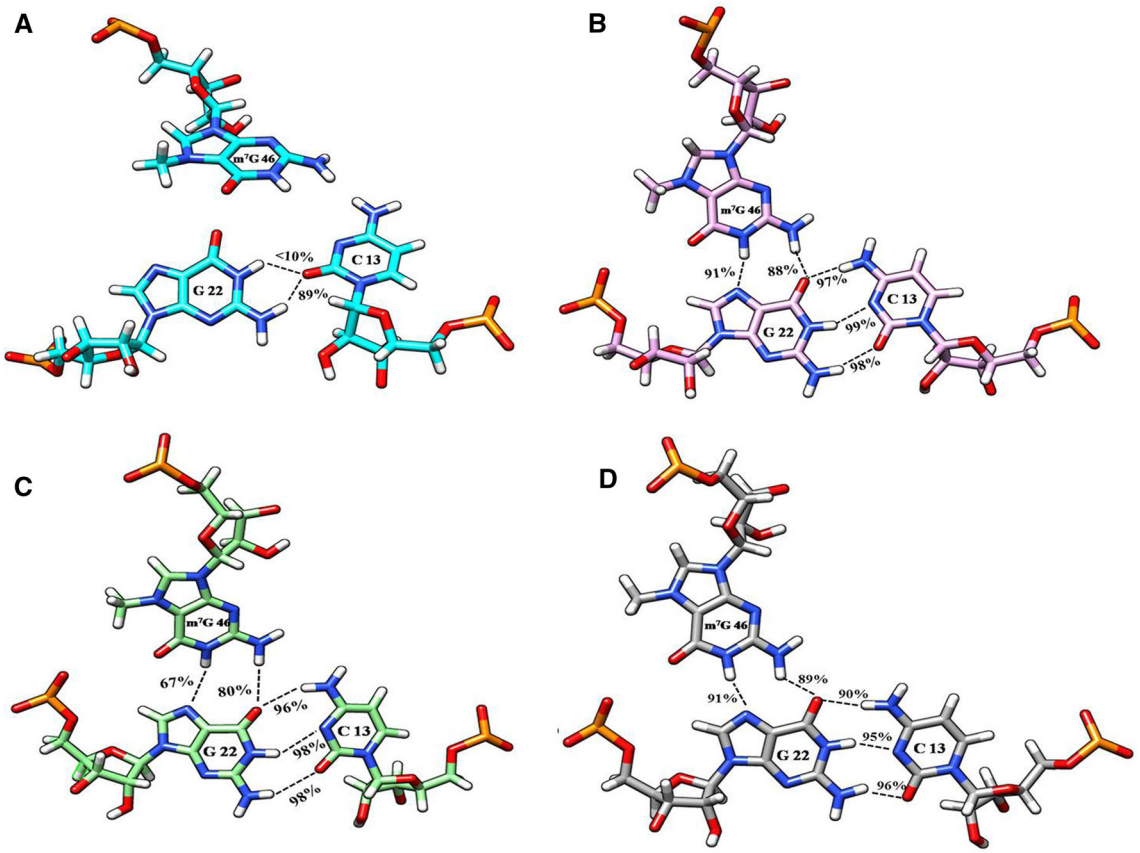

Fig. 6 The rearrangement of base triples m^7G46….[C13-G22]. **a** The base triples in the unmodified tRNA compared with **b** the base triples in m^2G containing tRNA, **c** the base triples in m^2_2G containing tRNA, and **d** the base triples in crystal structure with Mg^{2+} ions. HB % calculated from the 10-ns MD simulation for the base triples

unmodified guanosine (G) at the hinge region get stabilized by G18-C56 instead of G18-Ψ55, which may be due to a structural rearrangement observed during molecular dynamic simulation [50].

Root Mean Square Deviation (RMSD)

In order to get a rough estimate of the quality of the molecular dynamic simulation trajectory, the backbone root-mean-square deviation (RMSD) from the starting structure was calculated using PTRAJ module of AMBERTOOLS 10 and plotted using the commercially available *Sigma Plot 12.0* software. Figure 12 displays the time dependent root-mean-square deviation for all the three tRNA trajectories. The calculated RMSD of crystal structure remains in between 1.8 and 2.2 Å (Fig. 12). Root-mean-square deviation of tRNA with m^2G at the 26th position fluctuates around 2.3 Å and do not drift towards higher values during the simulation period (Fig. 12). Mobility of core residues continues to be close toward those derived from the crystal data. Transfer RNA having m^2_2G at the 26th position was also found to be stable with the values ranging from 2.5 to 2.7 Å compared with the tRNA containing guanosine (Fig. 12). The RMSD of tRNA containing m^2G is less compared to tRNA containing m^2_2G in the hinge region (Fig. 12). This could be because of the steric interactions between dimethylated groups of m^2_2G with A44. The cyan color line corresponds to the RMS deviations calculated for entire tRNA without any modification in the hinge region (Fig. 12). Such fluctuations may be due to displacement observed in base triples, resulting in loss of base stacking interactions and U turn motif of anticodon loop and TΨC loop. RMSD fluctuations revealed that the modifications at 26th position play an important role to stabilize the tertiary structure of tRNA.

Root Mean Square Fluctuation (RMSF)

Per residue root-mean-square fluctuation for the entire tRNA with and without modifications at the hinge region (the 26th position) has also been calculated and shown in Fig. 13. By observing fluctuations at the level of nucleotide

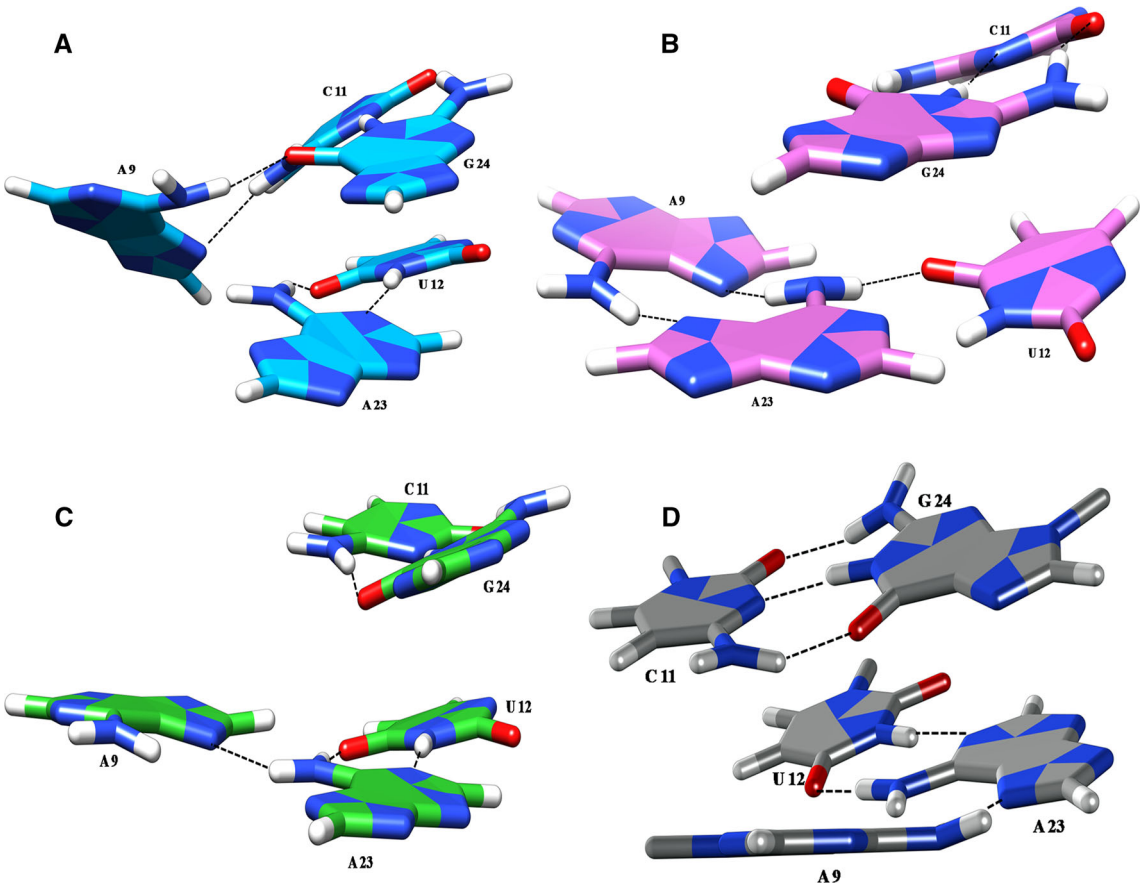

Fig. 7 The rearrangement of base triples A9….[U12-A23] and hydrogen-bonding interaction formed between adjacent base pairs, when **a** G at the 26th position in tRNA, **b** m^2G at the 26th position in tRNA **c** m_2^2G at the 26th position in tRNA, and **d** crystal structure with Mg^{2+} ions

residues, one can find that the deviation is maximum for the initial bases of acceptor arm, and some bases of anticodon stem loop and TΨC loop (Fig. 13). The significant deviation has been observed in the bases positioning from the 26th to 34th of the anticodon stem loop. Such large deviation in root-mean-square fluctuation may be due to displacement observed in base triples, resulting in loss of base stacking interactions and U turn motif of anticodon loop (Fig. 13). Though, the analogous (Ψ55) N3-H…O2P(A58) interaction in the thymine loop disrupt after 1400 ps due to dynamical rearrangements, which may cause large deviation in root-mean-square fluctuation in TΨC loop (base 58th to 61st). This result shows that the overall preservation of structure in the acceptor arm and D-stem of the tRNA has been maintained in the presence of modified bases at the hinge region. This signifies the movements in the TΨC loop and anticodon stem which mainly account for the drifts seen in all atom RMSF profile. Compared with crystal structure data [8], fluctuations in acceptor arm, D-arm, and anticodon loop remain fairly close, but relatively larger variation is observed in thymine loop.

Mg^{2+} Ions Coordination in Yeast $tRNA^{Phe}$

The two Mg^{2+} ions present in the D loop of crystal structure [8] coordinated by three consecutive phosphate groups of residues 19, 20, and 21 (Fig. 14a, b). One of the Mg^{2+} ions interacts with phosphate oxygen atoms of 20 and 21 nucleotides, while the other is coordinated with phosphate oxygen of base 19. Water molecule in its coordination shell gets stabilized by forming hydrogen bond with the phosphate oxygen of U59 base. During molecular dynamic simulation, phosphate oxygen of G15, G19, two water molecules, and oxygen atoms of residues G20 and C60 fulfill the octahedral geometry of Mg^{2+} ion located in the D loop (Fig. 14a1) as observed in crystal structure [8].

The magnesium ion located in the D loop (Fig. 14c) is stabilized by hydrogen bonding through its coordination sphere to four phosphate oxygen atoms of bases 8, 9, 11 and 12. This magnesium ion is held by total 6 hydrogen bonds from its coordinated water molecules to phosphate oxygen atoms of U8 and C12 nucleotides, respectively. The coordination of Mg^{2+} ion (Fig. 14b1) is in agreement

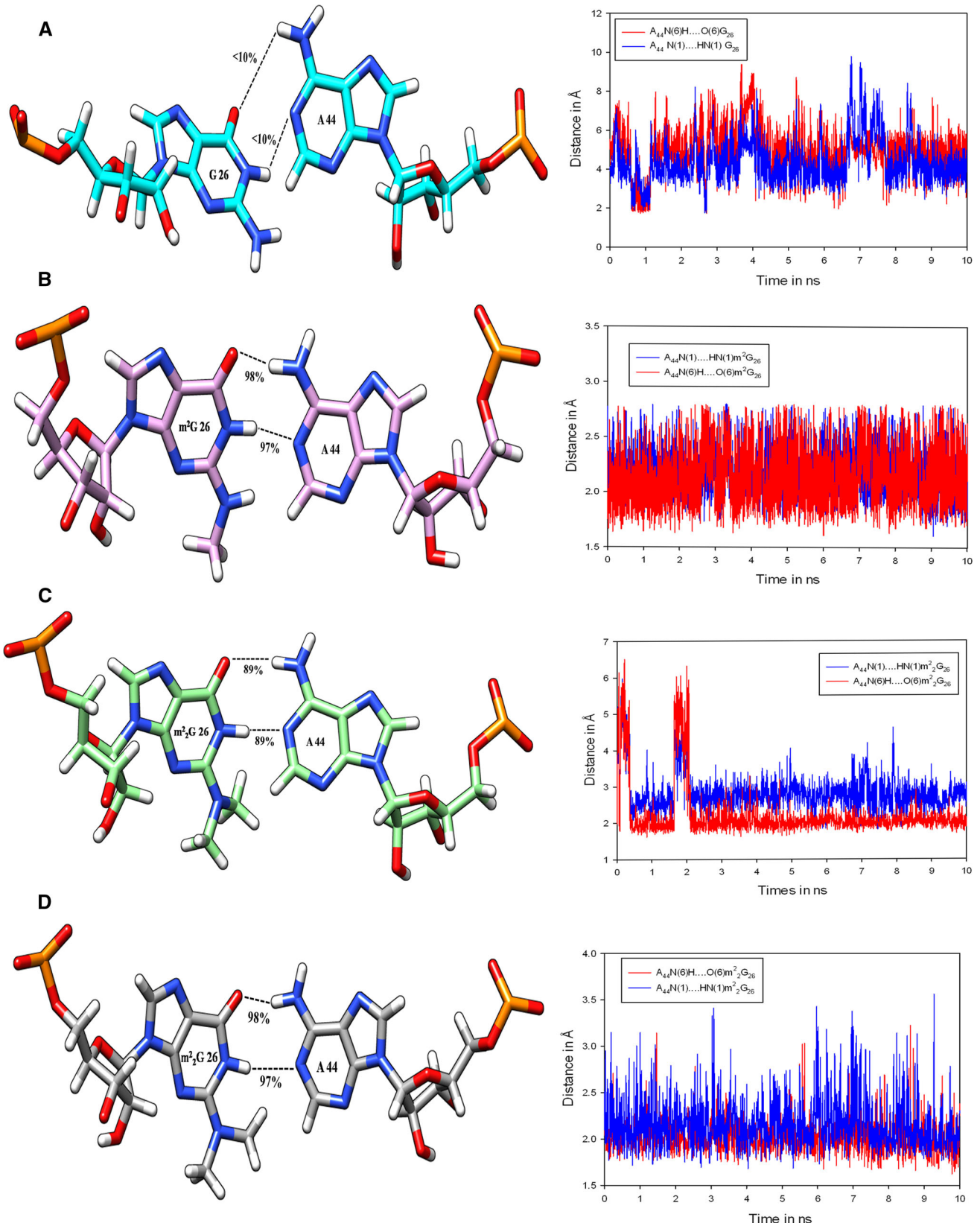

Fig. 8 Base pairing and HB % calculated from the 10-ns molecular dynamic simulation for the tertiary base pair present in the hinge region of tRNA, between **a** G26:A44, **b** m^2G26:A44, **c** m^2_2G26:A44 and **d** m^2_2G26:A44 in crystal structure with Mg^{2+} ions. The plot monitoring the hydrogen bond interactions between N1-H….N1 (*blue*) and O6….H-N6 (*red*) for the respective tertiary base pairs (Color figure online)

with crystal structure (Fig. 14b) during molecular dynamic simulation period.

The anticodon loop also contains a magnesium ion as shown in Fig. 14d. This magnesium ion is coordinated by phosphate oxygen of the 37th base and five oxygen atoms from water molecules (Fig. 14d). The Mg^{2+} ion forms water-mediated bonds with residues 32 and 39 of anticodon arm (Fig. 14d). Figure 14c1, d1 obtained from MD simulation show three phosphate oxygen atoms and three water molecules in the coordination sphere of Mg^{2+} ion. These magnesium ions show additional interactions with phosphate oxygen atoms compared to crystal conformers [8]. During MD simulation, some regions of tRNA (residue 55–62, 68–72) fluctuate more in the absence of Mg^{2+} ions compared to simulations performed in the presence of Mg^{2+} ions as can be seen in the RMSF graph (Fig. 13).

Fig. 11 Base pairing from the 10-ns molecular dynamic simulation ▶ for the tertiary base pair present between **a** G18: Ψ55 in tRNA with unmodified guanosine (G) at 26th position, **b** G18: Ψ55 in tRNA with m^2G at 26th position, **c** G18: Ψ55 in tRNA with m^2_2G at 26th position, **d** G18: Ψ55 in crystal structure. The plot monitoring the hydrogen bond interaction between N(1)H….O(4) (*blue*) and N(2)H….O (4) (*red*) for the respective tertiary base pair (Color figure online)

Single-Point Energy and MEPs Calculations of G/m^2G/m^2_2G26:A44

The base-paired structures namely, G26:A44 (Fig. 15a), m^2G26:A44 (Fig. 15b), m^2_2G26:A44 in the absence of Mg^{2+} (Fig. 15c) and m^2_2G26:A44 crystal structure with Mg^{2+} ions (Fig. 15d) have been extracted from the final MD simulated trajectories to investigate base-pairing interactions and energy differences. These isolated base-

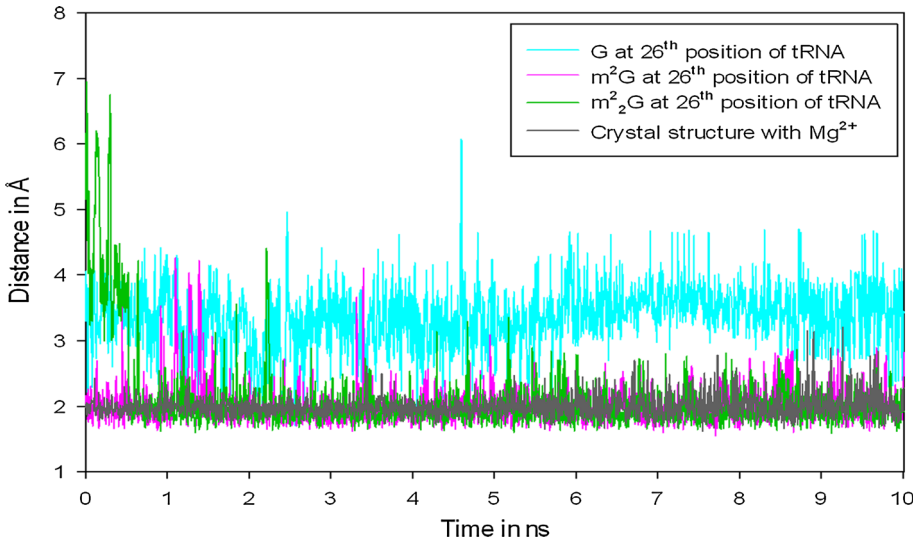

Fig. 9 Time course of hydrogen bond between (U33) N3-H…O2P (A36) describing the U-turn feature of anticodon loop. The *cyan color line* corresponds to guanosine at 26th position of tRNA, the *green colored line* corresponds to N^2-N^2 dimethylguanosine (m^2_2G) at 26th position of tRNA, the *magenta color* depicts N^2-methylguanosine (m^2G) at 26th position of tRNA while the *gray color* depicts N^2-N^2 dimethylguanosine (m^2_2G) at 26th position in the presence of Mg^{2+} ions in crystal structure (Color figure online)

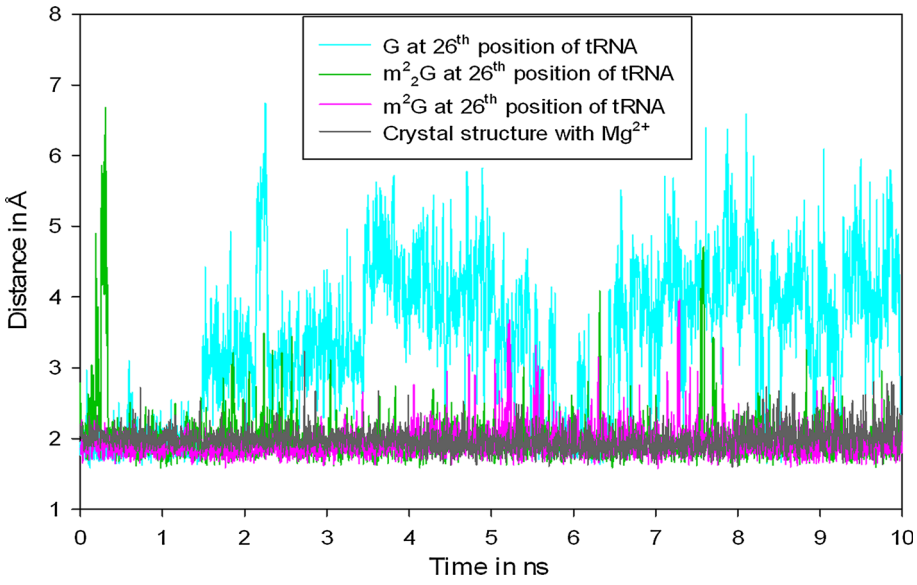

Fig. 10 Time course of hydrogen bond between (Ψ55) N3-H…O2P (A58) describing the U-turn feature of thymine loop. The *cyan color line* corresponds to guanosine at 26th position of tRNA, the *green colored line* corresponds to N^2-N^2 dimethylguanosine (m^2_2G) at 26th position of tRNA, the magenta color depicts N^2-methylguanosine (m^2G) at 26th position of tRNA while *gray color* depicts N^2-N^2 dimethylguanosine (m^2_2G) at 26th position in the presence of Mg^{2+} ions in crystal structure (Color figure online)

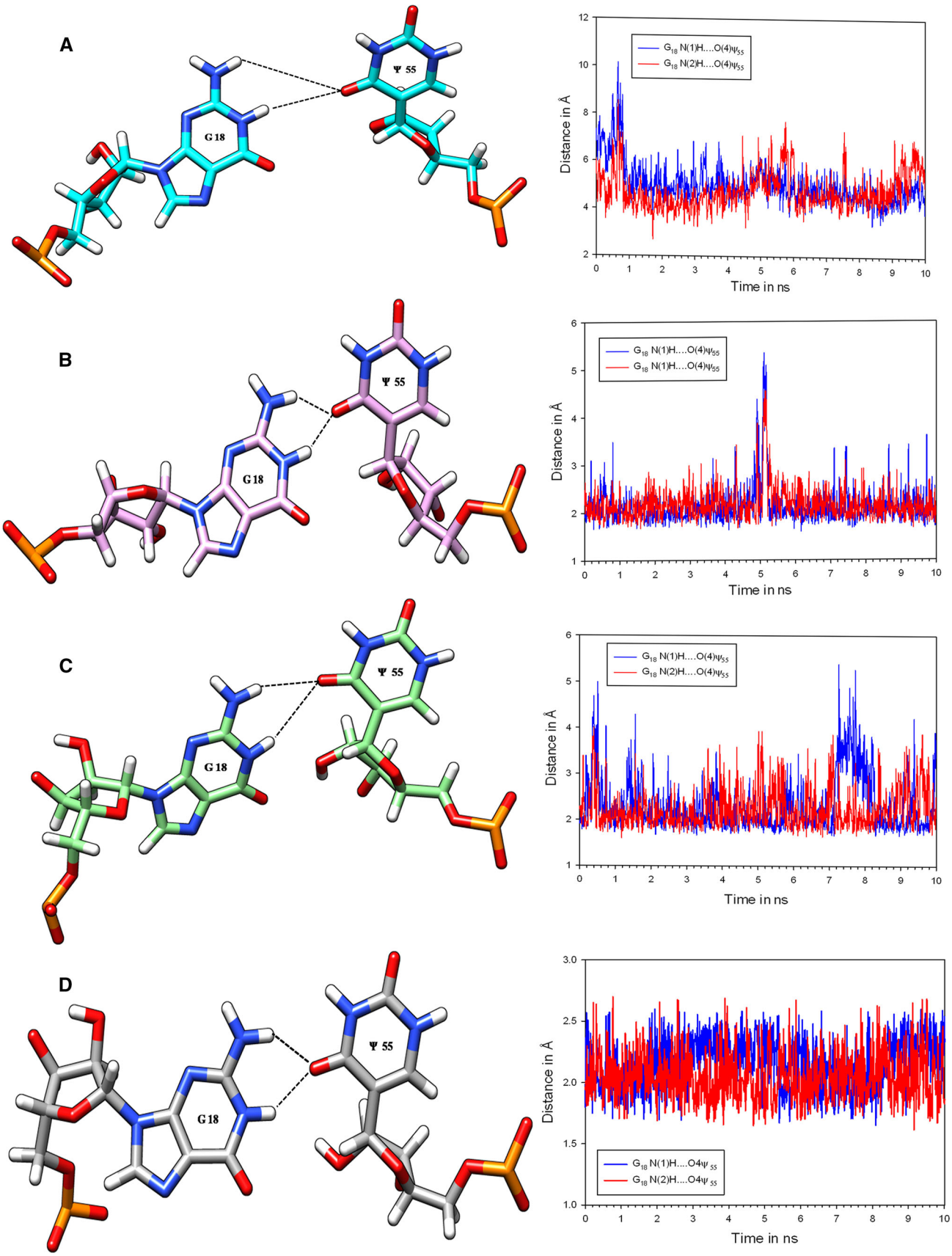
A
G 18
Ψ 55
Distance in Å
Time in ns
G18 N(1)H....O(4)ψ55
G18 N(2)H....O(4)ψ55
B
G 18
Ψ 55
Distance in Å
Time in ns
G18 N(1)H....O(4)ψ55
G18 N(1)H....O(4)ψ55
C
G 18
Ψ 55
Distance in Å
Time in ns
G18 N(1)H....O(4)ψ55
G18 N(2)H....O(4)ψ55
D
G 18
Ψ 55
Distance in Å
Time in ns
G18 N(1)H....O4ψ55
G18 N(2)H....O4ψ55

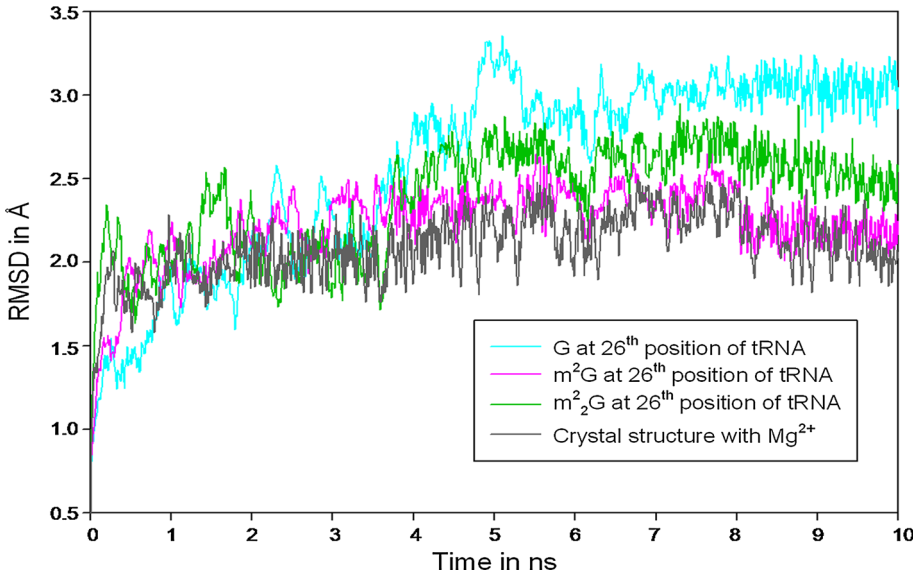

Fig. 12 Time course of the RMS deviations from the starting structure. The *cyan color line* corresponds to guanosine at 26th position of tRNA, the *green colored line* corresponds to N^2-N^2 dimethylguanosine (m^2_2G) at 26th position of tRNA, the magenta color depicts N^2-methylguanosine (m^2G) at 26th position of tRNA while *gray color* depicts N^2-N^2 dimethylguanosine (m^2_2G) at 26th position in the presence of Mg^{2+} ions in crystal structure (Color figure online)

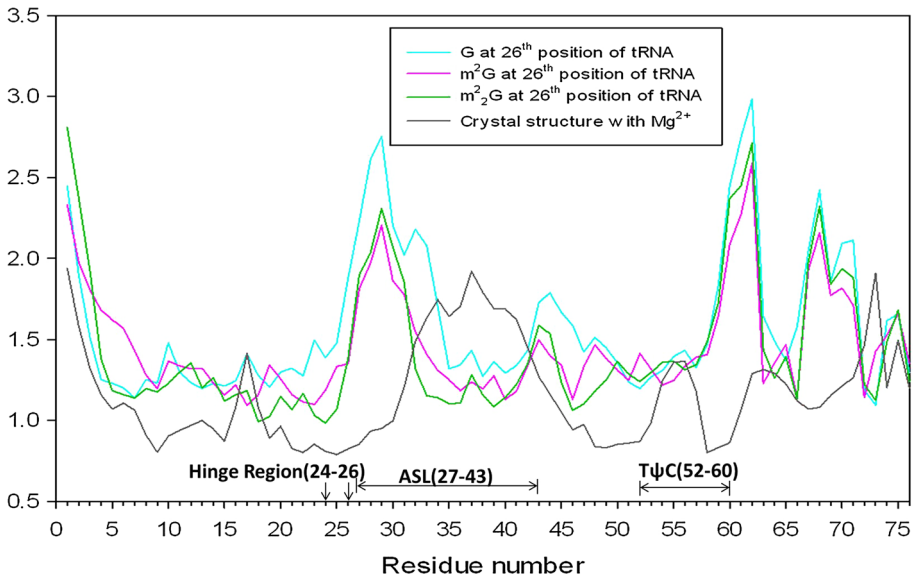

Fig. 13 Comparison of per residue root-mean-square fluctuations (RMSF) for entire tRNAs in the presence and the absence to Mg^{2+} over 10-ns time scale

paired structures are then subjected for single-point energy calculation and MEPs by means of HF-SCF (6-31G** basis set) similar to our earlier study [43]. The direct energy comparison (Table 1) has been made between all the base pair models instead of relative energies due to differences in the atom numbers. The MEPs and calculated energies (Table 1) show that m^2_2G26:A44 with and without Mg^{++} ions (Fig. 15c, d) are relatively stable compared to m^2G26:A44 (Fig. 15b) and G26:A44 (Fig. 15a), respectively. Two electrostatic potential tunnels have been observed in case of m^2G26:A44 (Fig. 15b). The N^2-methylguanosine (m^2G26:A44) (Fig. 15b) prefers *s-trans* or "proximal" conformation as observed in earlier studies [13, 14]. Similarly, one potential tunnel has been found in case of m^2_2G:A in the absence of Mg^{2+} ions. However, such electrostatic potential tunnels have not been observed in case of G26:A44 and m^2_2G26:A44 in the presence of Mg^{2+} ions. The crystal structure of yeast $tRNA^{Phe}$ containing m^2_2G26:A44 does not show hydrogen-bonding interactions at hinge region [8].

Discussion

Present 10-ns molecular dynamic simulations of $tRNA^{Phe}$ with nucleosides $m^2G/m^2_2G/G$ at the 26th position depict most of the significant interactions contributing to the stability and molecular architecture. From the biochemical and biophysical points of view, molecular dynamic simulations of tRNA molecule offer the opportunity to explore the stability of base triples and tertiary base pairs, which are primarily present in the core of the tRNA molecule

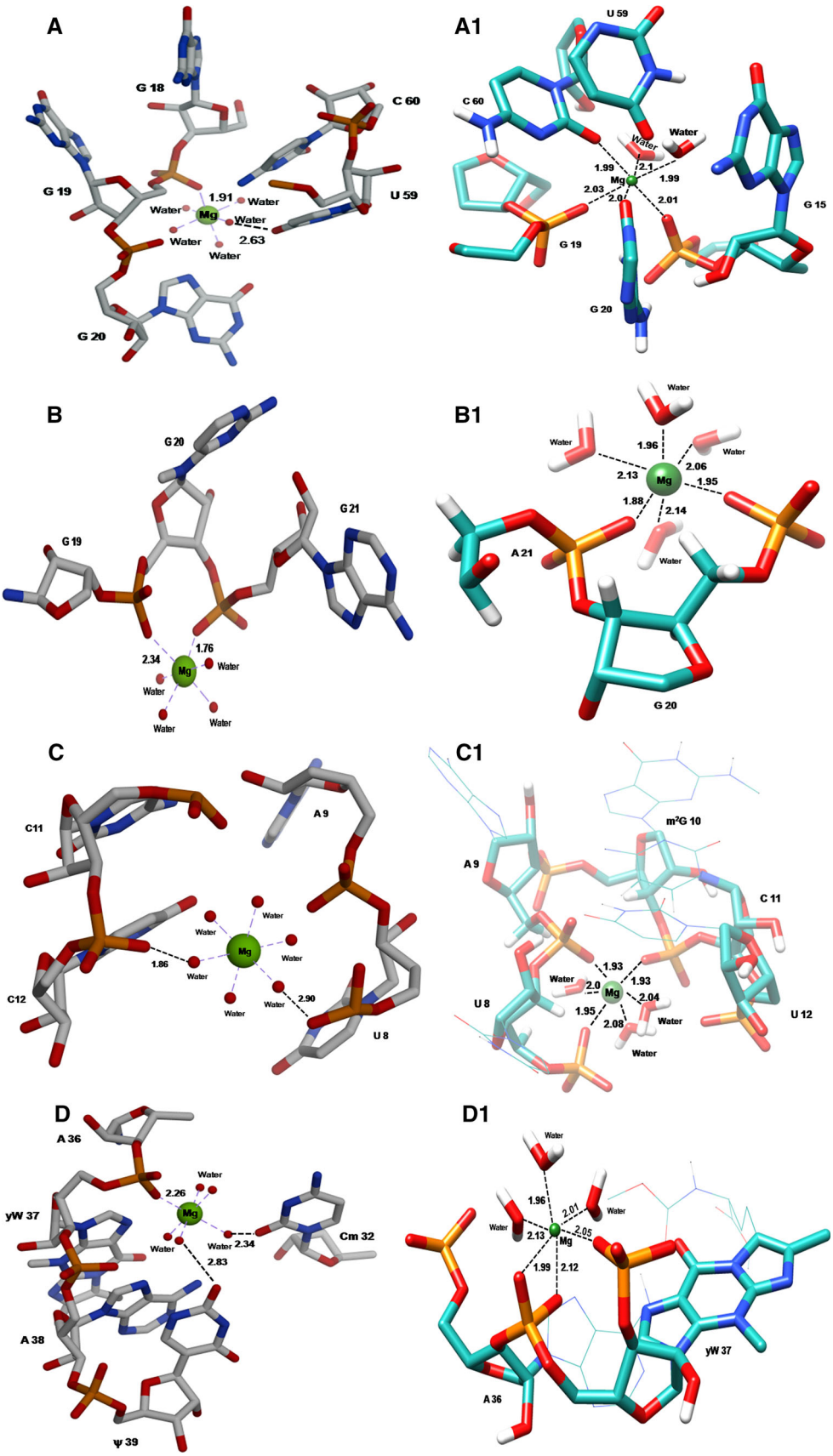

Fig. 14 Mg^{2+} ions (*green*) coordination observed in crystal structure (**a**–**d**) and molecular dynamic simulation (**a1**–**d1**) (Color figure online)

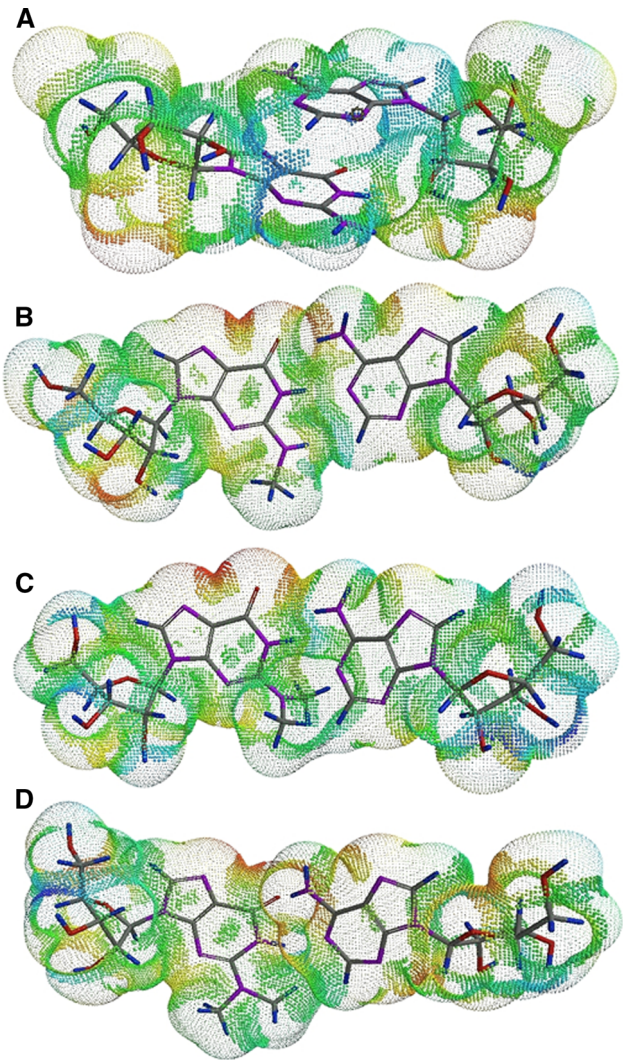

Fig. 15 Showing MEPs calculations of base pair models **a** G26:A44, **b** m^2G26:A44, **c** m_2^2G26:A44, **d** m_2^2G26:A44 crystal structure with Mg^{++} ions extracted from the final MD simulated trajectories

[50]. We show that in the presence of unmodified guanosine, the overall tertiary interactions of tRNA are essentially not the same as those of m^2G and m_2^2G containing tRNAs. This difference in tertiary interactions results in structural rearrangement, which may be due to intrinsic factors associated with the weak hydrogen-bonding patterns observed in the base triples of the tRNA molecule. Interestingly, similar type of structural rearrangement of base triples had also been observed in $tRNA^{Asp}$ in the presence of guanosine at the 26th position [50]. The interactions of tertiary base pairs found in the deep groove exhibit different levels of stability, and could be responsible for complete loss of interactions of the three base triples to a reversible interchange of hydrogen-bonding patterns for the G45…[G10-U25] [50]. Such liability in MD simulation may be due to, U11-A24 base pair of the D-stem which does not participate in the triple interaction and results in structural rearrangement by introducing a break in the stack of four base triples [50]. Byrne and coworkers in 2010 also showed the formation of the base triples composed of G10, C25, and G44, while A26 was left unpaired in unmodified *E. coli* $tRNA^{Phe}$ [54]. The unmodified $tRNA^{Phe}$ bound to MiaA (PDB IDs 2ZM5 and 2ZXU) shows a base triple between C11, G24 and G44 whereas a second base pair is formed between C25 and G10 while A26 is left unpaired [54]. Neither of this base triples arrangement is similar to that observed in the present structure, thus signifying the remodeling of tRNA by ribosomes or proteins resulted in conformational changes which are facilitated by flexibility in the core of the tRNA [54]. Owing to such liability observed in base triple interactions may be partly related to the experimental difficulties involved in their detection.

Interestingly, during MD simulation tertiary base pairs of tRNAs with m^2G/m_2^2G at the hinge region were found to be more stable compared to that of unmodified guanosine (Fig. 8). On the other hand, in the absence of Mg^{2+} ions in $tRNA^{Asp}$, structural rearrangement of some tertiary interactions observed in the base triples, in the U-turn motif of anticodon loop and as well as in the TΨC loop as per earlier study [50]. The NMR derived anticodon loop of unmodified Anticodon Stem Loop (ASL) of *E. coli* $tRNA^{Phe}$ (PDB 1KKA) does not adopt the significant U-turn feature, but instead has an unusual conformation in which the anticodon loop has three nucleotides [55].

The calculated per residue RMSF shows large deviations for the initial bases of the acceptor arm, some bases of the anticodon stem loop and TΨC loop. The fluctuation seen in different parts of tRNA can be evaluated by comparing it with experimental results. The RMSF results are in agreement with the calculated B-factor, which also show considerable deviation for the anticodon loop and the acceptor stem extremity [50]. In particular, residues of TΨC loop (Ψ55, C56, and A57) were found to be more

Table 1 Energy differences obtained by single-point energy calculation over the base pair models of G26/m^2G26/m_2^2G26:A through ab initio HF method

Name of the molecule	HF-SCF (6-31G** basis set) (kcal/mol)	Figure
G: A	−1,249,198.8705	Figure 15a
m^2G: A	−1,273,689.2519	Figure 15b
m_2^2G: A	−1,298,136.0733	Figure 15c
m_2^2G: A with Mg^{++} ions	−1,298,151.9509	Figure 15d

mobile (Fig. 13) than in the crystals [50]. The fluctuation of D loop residues was in close agreement with the calculated experimental values [8]. The MEPs tunnels observed in case of m^2G26:A44 and m_2^2G26:A44 in the presence and the absence of Mg^{2+} ions revealed the importance of these modified bases to maintain rigidity/flexibility in the hinge region of $tRNA^{Phe}$.

Conclusion

We have examined the dynamic features of solvated $tRNA^{Phe}$ in the presence and the absence of modified bases, N^2-methylguanosine (m^2G), N^2-N^2 dimethylguanosine (m_2^2G) present at the hinge region of $tRNA^{Phe}$. Molecular dynamic simulations result revealed the structural stability in the presence of m^2G and m_2^2G at the 26th position of $tRNA^{Phe}$. The MD simulated $tRNA^{Phe}$ containing m^2G and m_2^2G along with their crystal conformer retains complex three-dimensional fold through tertiary interactions.

MD simulation of tRNA having unmodified guanosine at the 26th position shows structural rearrangement in the core of the tRNA molecule resulting in lack of base stacking interactions, U-turn feature of anticodon loop and TΨC loop. The stability between residues 26, 44, and 45 is important, as they are involved in the formation of tRNA kink between D-stem and anticodon stem, allowing the tRNA anticodon to bind at the mRNA codons as explained in earlier report [56]. Thus, the modified nucleic acid bases are involved in stabilization of the hinge region between the anticodon and D stems as proposed previously based on X-ray structure of yeast $tRNA^{Phe}$ [57–59]. Energy calculations and molecular electrostatic potential (MEPs) studies revealed the structural significance of tRNAs containing m^2G26 and m_2^2G26 compared to tRNAs with normal G. Hence, the modified nucleosides m^2G26 and m_2^2G26 may play their respective important roles to provide structural stability at the hinge region of $tRNA^{Phe}$ for smooth and in-phase protein biosynthesis process. Thus, these results could be useful to understand the role of methylated nucleosides on tRNA folding.

Acknowledgments K.D.S. is grateful to the University Grants Commission, New Delhi for the financial support under UGC-SAP Phase-II program sanctioned to the Dept. of Biochemistry, Shivaji University, Kolhapur. R.S.B. and P.M.F. are thankful to the UGC for providing fellowships under UGC-BSR scheme. The authors are thankful to the Computer Center, Shivaji University for providing computational facility.

References

1. Winkler, M. E. (1998). Genetics and regulation of base modification in the tRNA and rRNA of prokaryotes and eukaryotes. In H. Grosjean & R. Benne (Eds.), *Modification and editing of RNA* (pp. 441–470). Washington, DC: ASM Press.
2. Noon, K. R., Guymon, R., Crain, P. F., McCloskey, J. A., Thomm, M., Lim, J., & Cavicchioli, R. (2003). Influence of temperature on tRNA modification in Archaea: Methanococcoides burtonii (optimum growth temperature [T_{opt}], 23°C) and Stetteria hydrogenophila (T_{opt}, 95°C). *Journal of Bacteriology, 185*, 5483–5490.
3. Limbach, P. A., Crain, P. F., & McCloskey, J. A. (1994). Summary: The modified nucleosides of RNA. *Nucleic Acids Research, 22*, 2183–2196.
4. Limbach, P. A., Crain, P. F., Pomerantz, S. C., & McCloskey, J. A. (1995). Structures of post transcriptionally modified nucleosides from RNA. *Biochimie, 77*, 135–138.
5. Sprinzl, M., Horn, C., Brown, M., Ioudovitch, A., & Steinberg, S. (1998). Compilation of tRNA sequences and sequences of tRNA genes. *Nucleic Acids Research, 26*, 148–153.
6. Saenger, W. (1984). *In Principles of nucleic acid structure* (pp. 334–337). New York: Springer.
7. Auffinger, P. S., & Westhof, E. (1998). Effects of pseudouridylation on tRNA hydration and dynamics: A theoretical approach. In H. Grosjean & R. Benne (Eds.), *Modification and editing of RNA* (pp. 569–576). Washington DC: ASM Press.
8. Sussman, J. L., Holbrook, S. R., Warrant, R. W., Church, G. M., & Kim, S. H. (1978). Crystal structure of yeast phenylalanine transfer RNA. I. Crystallographic refinement. *Journal of Molecular Biology, 123*(4), 607–630.
9. Edqvist, J., Straby, K. B., & Grosjean, H. (1995). Enzymatic formation of N^2,N^2-dimethylguanosine in eukaryotic tRNA: Importance of the tRNA architecture. *Biochimie, 77*(1–2), 54–61.
10. Pallan, P. S., Kreutz, C., Bosio, S., Micura, R., & Egli, M. (2008). Effects of N^2,N^2-dimethylguanosine on RNA structure and stability: Crystal structure of an RNA duplex with tandem M22G: A pairs. *RNA, 14*, 2125–2135.
11. Boyle, J., Robillard, G. T., & Kim, S. H. (1980). Sequential folding of transfer RNA: A nuclear magnetic resonance study of successively longer tRNA fragments with a common 5′ end. *Journal of Molecular Biology, 139*, 601–625.
12. Rife, J. P., Cheng, C. S., Moore, P. B., & Strobel, S. A. (1998). N^2-methylguanosine is iso-energetic with guanosine in RNA duplexes and GNRA tetraloops. *Nucleic Acids Research, 26*, 3640–3644.
13. Bavi, R. S., Kamble, A. D., Kumbhar, N. M., Kumbhar, B. V., & Sonawane, K. D. (2011). Conformational preferences of modified nucleoside N^2-methylguanosine (m^2G) and its derivative N^2,N^2-dimethylguanosine (m_2^2G) occur at 26th position (Hinge region) in tRNA. *Cell Biochemistry and Biophysics, 61*, 507–521.
14. Bavi, R. S., Sambhare, S. B., & Sonawane, K. D. (2013). MD Simulation studies to investigate conformational behavior of modified nucleosides m^2G and m_2^2G present in tRNA. *Computational & Structural Biotechnology Journal, 5*, 1–8.
15. Ginell, S. L., & Parthasarathy, R. (1978). Conformation of N^2-methylguanosine, a modified nucleoside of tRNA. *Biochemical & Biophysical Research Communications, 84*, 886–894.
16. Bjork, G. R., & Kohli, J. (1990). Biological roles and function of modification. In C. W. Gehrke & C. T. Kuo (Eds.), *Chromatography and modification of nucleosides part B* (pp. 13–67). Amsterdam: Elsevier.
17. Muramatsu, T., Nishikawa, K., Nemoto, F., Kuchino, Y., Nishimura, S., Miyazawa, T., & Yokoyama, S. (1988). Codon and amino-acid specificities of a transfer RNA are both converted by a single post-transcriptional modification. *Nature, 336*(6195), 179–181.
18. Muramatsu, T., Yokoyama, S., Horie, N., Matsuda, A., Ueda, T., Yamaizumi, Z., et al. (1988). A novel lysine-substituted nucleoside in the first position of the anticodon of isoleucine tRNA

from *Escherichia coli*. *Journal of Biological Chemistry, 263*, 9261–9267.
19. Agris, P. F. (2004). Decoding the genome: A modified view. *Nucleic Acids Research, 32*(1), 223–238.
20. Bjork, G. R. (1995). Biosynthesis and function of modified nucleosides. In D. Soll & U. L. RajBhandary (Eds.), *tRNA: Structure, biosynthesis and function* (pp. 165–206). Washington, DC: American Society for Microbiology Press.
21. Agris, P. F. (1996). The importance of being modified: Roles of modified nucleosides and Mg^{2+} in RNA structure and function. *Progress in Nucleic Acids Research & Molecular Biology, 53*, 79–129.
22. Davis, D. R., Veltri, C. A., & Nielsen, L. (1998). An RNA model system for investigation of pseudouridine stabilization of the codon–anticodon interaction in tRNAHis and tRNATyr. *Journal of Biomolecular Structure & Dynamics, 15*, 1121–1132.
23. Durant, P. C., & Davis, D. R. (1999). Stabilization of the anticodon stem-loop of $tRNA^{Lys}$ by an A^{+}-C base-pair and by pseudouridine. *Journal of Molecular Biology, 285*(1), 115–131.
24. Murphy, F. V., Ramakrishnan, V., Malkiewicz, A., & Agris, P. F. (2004). The role of modifications in codon discrimination by tRNA(Lys)UUU. *Nature Structural Biology, 11*(12), 1186–1191.
25. Chen, Y., Sierzputowska-Gracz, H., Guenther, R., Everett, K., & Agris, P. F. (1993). 5-Methylcytidine is required for cooperative binding of magnesium (2^{+}) and a conformational transition at the anticodon stem-loop of yeast phenylalanine tRNA. *Biochemistry, 32*, 10249–10253.
26. Nobles, K. N., Yarian, C. S., Liu, G., Guenther, R. H., & Agris, P. F. (2002). Highly conserved modified nucleosides influence Mg^{2+} dependant tRNA folding. *Nucleic Acids Research, 30*, 4751–4760.
27. Maglott, E. J., Deo, S. S., Przykorska, A., & Glick, G. D. (1998). Conformational transitions of an unmodified tRNA: Implications for RNA folding. *Biochemistry, 37*, 16349–16359.
28. Roh, J. H., Briber, R. M., Damjanovic, A., Thirumalai, D., Woodson, S. A., & Sokolov, A. P. (2009). Dynamics of tRNA at different levels of hydration. *Biophysics Journal, 96*, 2755–2762.
29. Šponer, J., Banáš, P., Jurečka, P., Zgarbová, M., Kührová, P., Havrila, M., et al. (2014). Molecular dynamics simulations of nucleic acids from tetranucleotides to the ribosome. *Journal of Physical Chemistry Letters, 5*, 1771–1782.
30. Bock, L. V., Blau, C., Schröder, G. F., Davydov, I. I., Fischer, N., Stark, H., et al. (2013). Energy barriers and driving forces in tRNA translocation through the ribosome. *Nature Structural & Molecular Biology, 20*, 1390–1396.
31. Berendsen, H. J. C., Griegera, G. R., & Straatsma, T. P. (1987). The missing term in effective pair potentials. *Journal of Physical Chemistry, 91*, 6269–6271.
32. Allner, O., Nilsson, L., & Villa, A. J. (2012). Magnesium ion-water coordination and exchange in biomolecular simulations. *Journal of Chemical Theory & Computations, 8*, 1493–1502.
33. Perez, A., Marchan, I., Svozil, D., Sponer, J., Cheatham, T. E, I. I. I., Laughton, C. A., & Orozco, M. (2007). Refinement of the AMBER force field for nucleic acids: Improving the description of α/γ conformers. *Biophysics Journal, 92*, 3817–3829.
34. Darden, T., York, D., & Pedersen, L. (1993). Particle Mesh Ewald—an N.Log(N) method for Ewald sums in large systems. *Journal of Chemical Physics, 98*, 10089–10092.
35. Ryckaert, J. P., Ciccotti, G., & Berendsen, H. J. C. (1977). Numerical integration of the Cartesian equations of motion of a system with constraints: Molecular dynamics of *n*-Alkanes. *Journal of Computational Physics, 23*, 327–336.
36. Berendsen, H. J. C., Postma, J. P. M., Van Gunsteren, W. F., DiNola, A., & Haak, J. R. (1984). Molecular dynamics with coupling to an external bath. *Journal of Chemical Physics, 81*, 3684–3690.
37. Auffinger, P. S., Louise-May, S., & Westhof, E. (1995). Multiple molecular dynamics simulations of the anticodon loop of $tRNA^{Asp}$ in aqueous solution with counterions. *Journal of American Chemical Society, 117*, 6720–6726.
38. Auffinger, P. S., Louise-May, S., & Westhof, E. (1996). Hydration of C-H groups in tRNA. *Faraday Discussions*, *103*, 151–173.
39. Aduri, R., Psciuk, B. T., Saro, P., Taniga, H., Schlegel, H. B., & Santa Lucia, J, Jr. (2007). AMBER force field parameters for the naturally occurring modified nucleosides in RNA. *Journal of Chemical Theory and Computation, 3*, 1464–1475.
40. Case, D. A., Darden, T. A., Cheatham, T. E, I. I. I., Simmerling, C. L., Wang, J., et al. (2008). *AMBER 10*. San Francisco: University of California.
41. Kumbhar, N. M., & Sonawane, K. D. (2011). Iso-energetic multiple conformations of Hypermodified nucleic acid base wybutine (yW) which occur at 37(th) position in anticodon loop if tRNA (Phe). *Journal of Molecular Graphics and Modelling, 29*, 935–946.
42. Kumbhar, N. M., Kumbhar, B. V., & Sonawane, K. D. (2012). Structural significance of Hypermodified nucleic acid base hydroxywybutine (OHyW) which occur at 37th position in the anticodon loop of yeast tRNAPhe. *Journal of Molecular Graphics and Modelling, 38*, 174–185.
43. Kumbhar, B. V., Kamble, A. D., & Sonawane, K. D. (2013). Conformational preferences of modified nucleoside N(4)-acetylcytidine, ac4C occur at wobble 34th position in the anticodon loop of tRNA. *Cell Biochemistry and Biophysics, 66*, 797–816.
44. Sonavane, U. B., Sonawane, K. D., Morin, A., Grosjean, H., & Tewari, R. (1999). N(7)-protonation induced conformational flipping in Hypermodified nucleic acid bases N^6-(*N*-threonylcarbonyl) adenine and its 2-methylthio or *N*(6)-methyl-derivatives. *International Journal of Quantum Chemistry, 75*, 223–229.
45. Sonawane, K. D., Sonavane, U. B., & Tewari, R. (2000). Conformational flipping of the N(6) substituent in diprotonated N^6-(*N*-glycylcarbonyl) adenines: The role of N(6)H in purine-ring-protonated ureido adenines. *International Journal of Quantum Chemistry, 78*, 398–405.
46. Sambhare, S. B., Kumbhar, B. V., Kamble, A. D., Bavi, R. S., Kumbhar, N. M., & Sonawane, K. D. (2014). Structural significance of modified nucleosides k^2C and t^6A present in the anticodon loop of $tRNA^{Ile}$. *RSC Advances, 27*, 14176–14188.
47. Sonawane, K. D., & Smabhare, S. B. (2015). Influence of hypermodified nucleosides lysidine and t6A to recognize AUA codon instead of AUG: A molecular dynamics simulation study. *Integrative Biology,*. doi:10.1039/C5IB00058K.
48. Kamble, A. S., Kumbhar, B. V., Sambhare, S. B., Bavi, R. S., & Sonawane, K. D. (2015). Conformational preferences of modified nucleoside 5-taurinomethyluridine, sm^5U occur at 'wobble' 34th position in the anticodon loop of tRNA. *Cell Biochemistry Biophysics, 71*, 1589–1603.
49. Kamble, A. S., Sambhare, S. B., Fandilolu, P. M., & Sonawane, K. D. (2015). Structural significance of modified nucleoside 5-taurinomethyl-2-thiouridine, τm^5s^2U found at 'wobble' position in anticodon loop of Human mitochondrial $tRNA^{Lys}$. *Structural Chemistry,*. doi:10.1007/s11224-015-0642-4.
50. Auffinger, P. S., Louise-May, S., & Westhof, E. (1999). Molecular dynamics simulation of solvated yeast tRNA (Asp). *Biophysics Journal, 76*, 50–64.
51. Quigley, G. J., & Rich, A. (1976). Structural domains of transfer RNA molecules. *Science, 194*, 796–806.
52. Kim, S. H., Suddath, F. L., Quigley, G. J., McPherson, A., Sussman, J. L., Wang, A. H., et al. (1974). Three-dimensional tertiary structure of yeast phenylalanine transfer RNA. *Science, 185*, 435–440.
53. Rich, A., & RajBhandary, U. L. (1976). Transfer RNA: Molecular structure, sequence, and properties. *Annual Review in Biochemistry, 45*, 805–860.

54. Byrne, R. T., Konevega, A. L., Rodnina, M. V., & Antson, A. A. (2010). The crystal structure of unmodified $tRNA^{Phe}$ from *Escherichia coli*. *Nucleic Acids Research, 38*, 4154–4162.
55. Cabello-Villegas, J., Winkler, M. E., & Nikonowicz, E. P. (2002). Solution structure of the unmodified anticodon stem-loop from *E. colli* tRNA (Phe). *Journal of Molecular Biology, 319*, 1015–1034.
56. Valle, M., Zavialov, A., Li, W., Stagg, S. M., Sengupta, J., Nielsen, R. C., et al. (2003). Incorporation of aminoacyl-tRNA into the ribosome as seen by cryo-electron microscopy. *Nature Structural Biology, 10*(11), 899–906.
57. Ladner, J. E., Jack, A., Robertus, J. D., Brown, R. S., Rhodes, D., Clark, B. F. C., & Klug, A. (1975). Structure of yeast phenylalanine transfer RNA at 2.5 Å resolution. *Proceedings of the National Academy of Science USA, 72*, 4414–4418.
58. Quigley, G. J., Wang, A. H. J., Seeman, N. C., Suddath, F. H., Rich, A., Sussman, J. L., & Kim, S. H. (1975). Hydrogen bonding in yeast phenylalanine transfer RNA. *Proceedings of the National Academy of Science USA, 72*, 4866–4870.
59. Steinberg, S., & Cedergren, R. (1995). A correlation between N^2-dimethylguanosine presence and alternate tRNA conformers. *RNA, 1*, 886–891.